

Supporting Information

Pulsed Electrical Stimulation Enhances Body Fluid Transport for Collagen Biomineralization

Doyoon Kim,^{1,§} Byeongdu Lee,² Brittany P. Marshall,³ Eunyoung Jang,¹ Stavros Thomopoulos,³
and Young-Shin Jun^{1,*}

¹ *Department of Energy, Environmental & Chemical Engineering, Washington University, St. Louis, Missouri 63130, United States*

² *X-ray Science Division, Argonne National Laboratory, Argonne, Illinois 60439, United States*

³ *Department of Orthopedic Surgery, Department of Biomedical Engineering, Columbia University, New York, New York 10032-3072, United States*

E-mail: ysjun@seas.wustl.edu

<http://encl.engineering.wustl.edu/>

ACS Applied Bio Materials

*To Whom Correspondence Should be Addressed

§Current address: Department of Civil and Environmental Engineering, Massachusetts Institute of Technology, Cambridge, MA 02139, USA

This supporting information includes 1 table, 5 figures and 10 pages.

Table S1. Concentrations (mM) of ionic components of simulated body fluids and human blood plasma.

Solutions	Na ⁺	K ⁺	Mg ²⁺	Ca ²⁺	Cl ⁻	HCO ₃ ⁻	HPO ₄ ²⁻	SO ₄ ²⁻	Ref.
1xSBF	142.0	5.0	1.5	2.5	147.8	4.2	1.0	0.5	²⁷
2.5xSBF	142.0	8.0	1.5	6.3	155.3	4.2	2.5	0.5	
Human blood plasma	142.0	5.0	1.5	2.5	103.0	27.0	1.0	0.5	²⁹

* The pH of the 2.5xSBF was adjusted to 7.4 with 50 mM of Tris ((CH₂OH)₃CNH₂) and 1 N HCl. In 2.5xSBF, 10 mg L⁻¹ polyaspartic acid was also added.

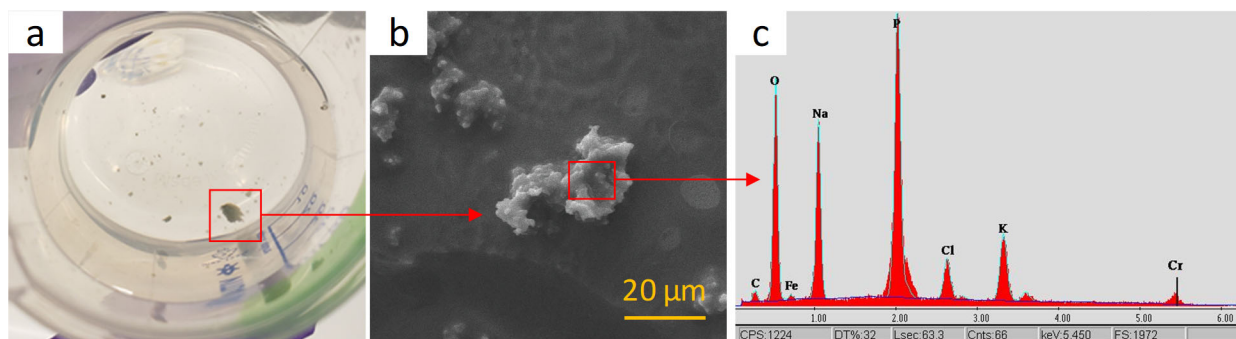


Figure S1. Secondary precipitates from dissolution of anode at amplitude of 3V. (a) Green precipitates formed after 2 h application of pulsed stimulation at 3 V amplitude (1 Hz frequency and 100 ms pulse width) in phosphate buffered saline. (b–c) SEM-EDX analysis shows that the precipitates contained Fe and Cr which were released from the dissolution of stainless steel anode. Note that the experimental conditions for the pulsed electrical stimulation in this study (40–200 mV, 48 h) did not induce any dissolution of the anode.

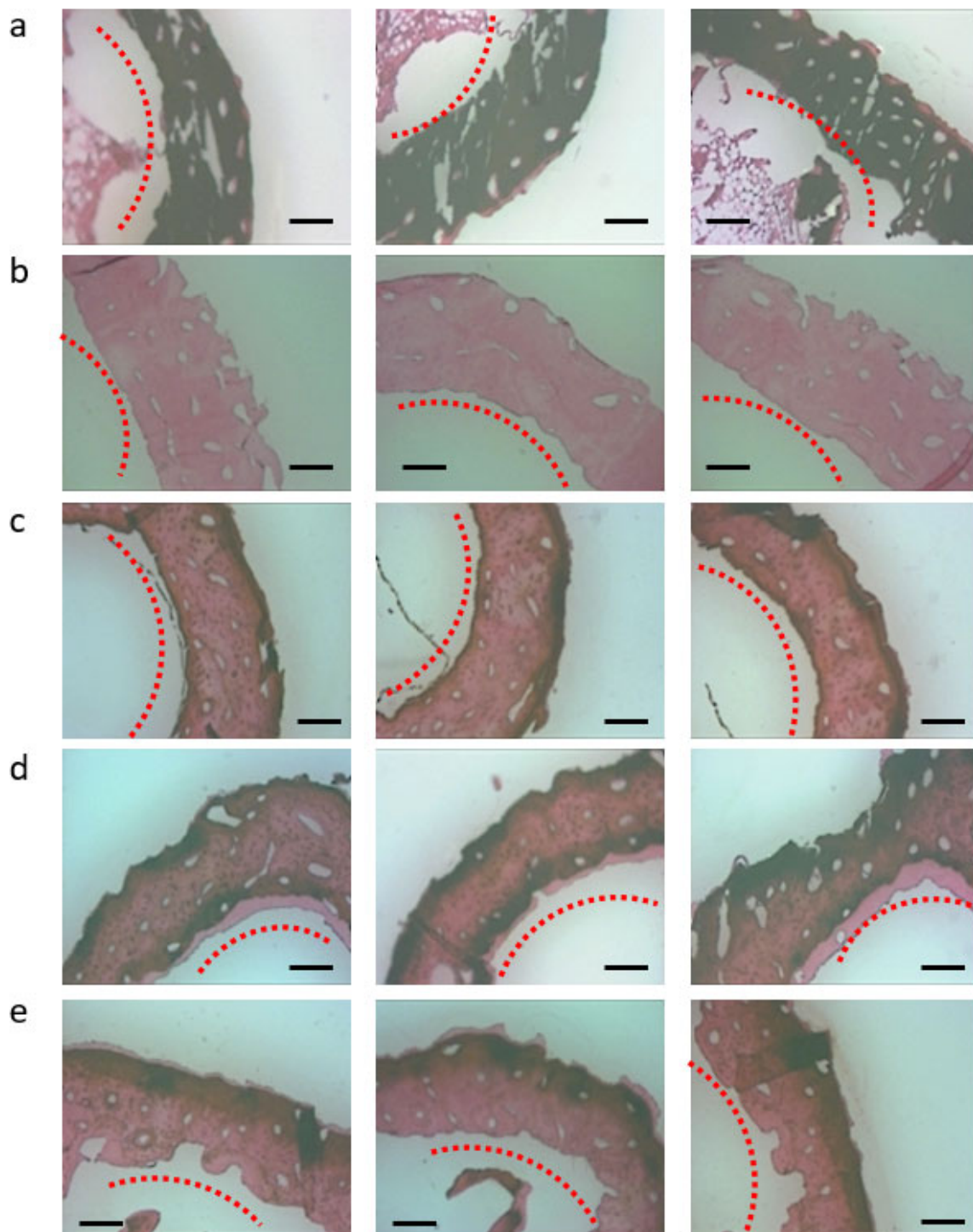


Figure S2. Optical images of cross-sections (5 μm thick) of collagen scaffolds. Dotted lines indicate the outlines of innermost surfaces. Samples were stained with von Kossa's (gray: mineral) and Goldner's trichrome (pink: collagen) methods. **(a)** Fresh fibular bone. **(b)** Demineralized fibular bone **(c–e)** Collagen mineralized for 48 h under pulsed electrical stimulation. **(c)** Control without stimulation. **(d)** Cathode. **(e)** Anode. Scale bars are 100 μm .

Note S1. Small-angle X-ray scattering/wide-angle X-ray diffraction data collections and analyses

Small-angle X-ray scattering (SAXS) measurements were conducted on collagen at different time intervals during its *in situ* mineralization. Samples were removed from the electrode and then placed onto a SAXS sample stage. For each SAXS scan, the sample was exposed to a 13.3 keV X-ray beam for 1 second. The beam was 150 μm (horizontal dimension, parallel to the long direction of the collagen) \times 40 μm (vertical dimension, perpendicular to the long direction of the collagen). To minimize the effect of spatial inhomogeneity on data statistics (Figure S3), each sample was scanned five times horizontally (along the fibrillar direction of the collagen), moving sample stage by 0.2 mm per scan. Then the average intensity was taken from the five scans. From the 2-dimensional scattering intensity images obtained from the detector (2M Pilatus), 1-dimensional scattering intensities, $I(q)$, were extracted by averaging the sector along the vertical lines, which was perpendicular to the fibrillar direction (Figure S3). From the sector averaged 1-dimensional $I(q)$, the increasing SAXS intensity during nucleation was quantified and the morphology of newly formed particles was evaluated without interference by peaks coming from the periodicity (~ 67 nm) of the collagen gap and hole regions. The distance from the sample to the SAXS detector was 2 m, which provided a range of 0.0017–0.53 \AA^{-1} for the scattering vector, q . Silver behenate powder was used as the q calibration standard, and $I(q)$ was normalized by the incident beam intensities. To compare absolute SAXS intensities collected from different measurements, the intensities were calibrated using a reference glassy carbon standard sample. The SAXS intensities were corrected by subtracting the intensity of air, measured by scanning the empty sample holder.

Further SAXS data analyses were conducted using the 1-dimensional horizontal cut data. Total particle volume was estimated from the linear relationship with invariant values, $Q =$

$\frac{1}{2\pi^2} \int q^2 I(q) dq$. The integration was performed over a limited q range of 0.0017–0.3 Å⁻¹, due to the relatively high noise in larger q regions. This Q value indicates the total scattering amount, and thus is proportional to the particle number concentration, $N_c = \frac{Q}{r_e^2 \Delta\rho^2 V}$, when the particle morphology is uniform.^{1,2} Here r_e and V respectively represent the classical electron radius (2.818 fm) and the volume of a particle. $\Delta\rho$ is the difference in electron densities between particles and water ($\Delta\rho = 6.12 \times 10^{23}$ cm⁻³; particles were assumed to be hydroxyapatite crystals and surrounded by water in collagen matrices).³ The Modeling II tool of the IRENA package written in IGOR Pro (WaveMetrics Inc.) was provided by APS and used to fit the SAXS pattern to evaluate the particle morphology. Because the morphology of individual particles was relatively uniform, a constant V was calculated. The volume fraction of minerals in collagen was obtained by $f_v = V \times N_c$. Details about the models used in the package are well described elsewhere.^{3,4}

Similarly, to identify the CaP phases during collagen mineralization, *in situ* wide angle X-ray diffraction (WAXD) data was collected at APS sector 11-ID-B. Every two hours during the mineralization, collagen samples were exposed to a 58.66 keV X-ray beam for 10 seconds at a 95 cm distance between the sample and a Perkin Elmer amorphous silicon detector. Due to the larger size of beam (500 μm × 500 μm) for WAXD than for SAXS, one scan spot of each sample was sufficient to provide good statistics. The 2-dimensional intensities were averaged over the q range along the radial direction to produce 1-dimensional intensities $I(q)$, using GSAS-II.⁵ Cerium dioxide was used as the calibration standard.

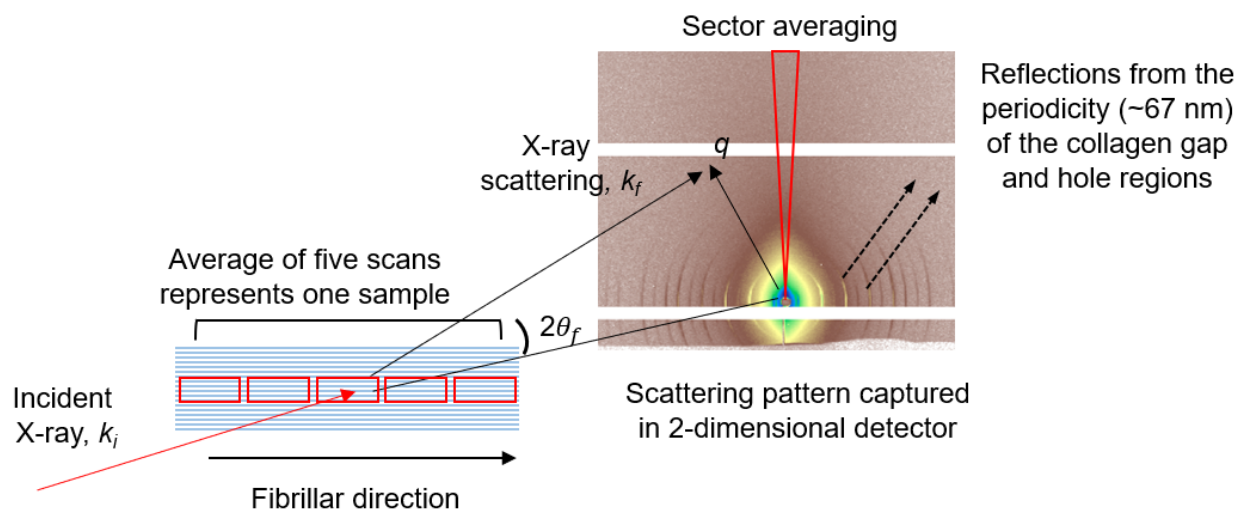


Figure S3. A schematic illustration of SAXS data collection. k_i and k_f are the incident and scattered wave vectors, respectively, and $2\theta_f$ is the exit angle of the X-rays. Five positions (red rectangles) of a sample along the fibrillar direction were scanned, and the scattered X-ray patterns were captured by a 2-dimensional detector. A selected sector of the detector along the vertical direction was analyzed as described in Note S1.

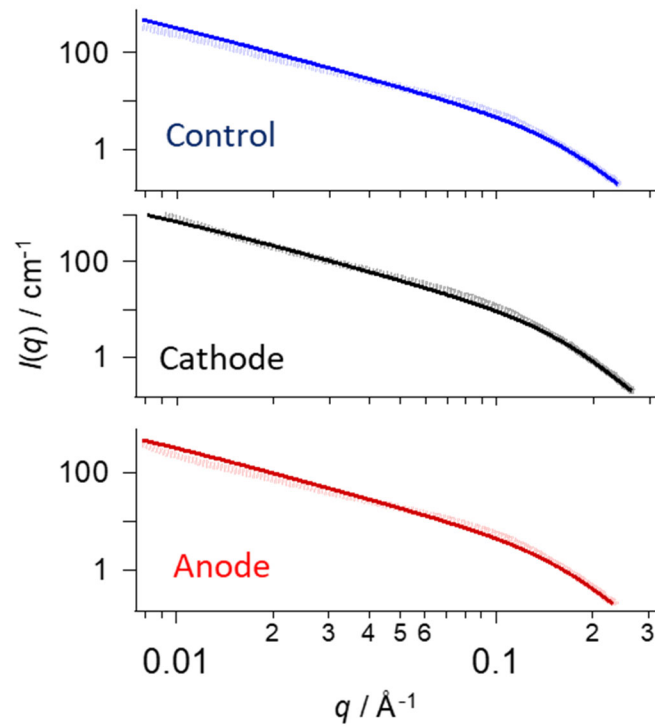


Figure S4. Background subtracted SAXS patterns for fitting the morphology of nuclei. The background intensity from an unmineralized collagen specimen was subtracted from the data in Figure 1a of the main text (dotted lines). Solid lines show the fitting results, indicating a disc-shaped nucleus (1.7 nm thick and 34 nm in diameter).

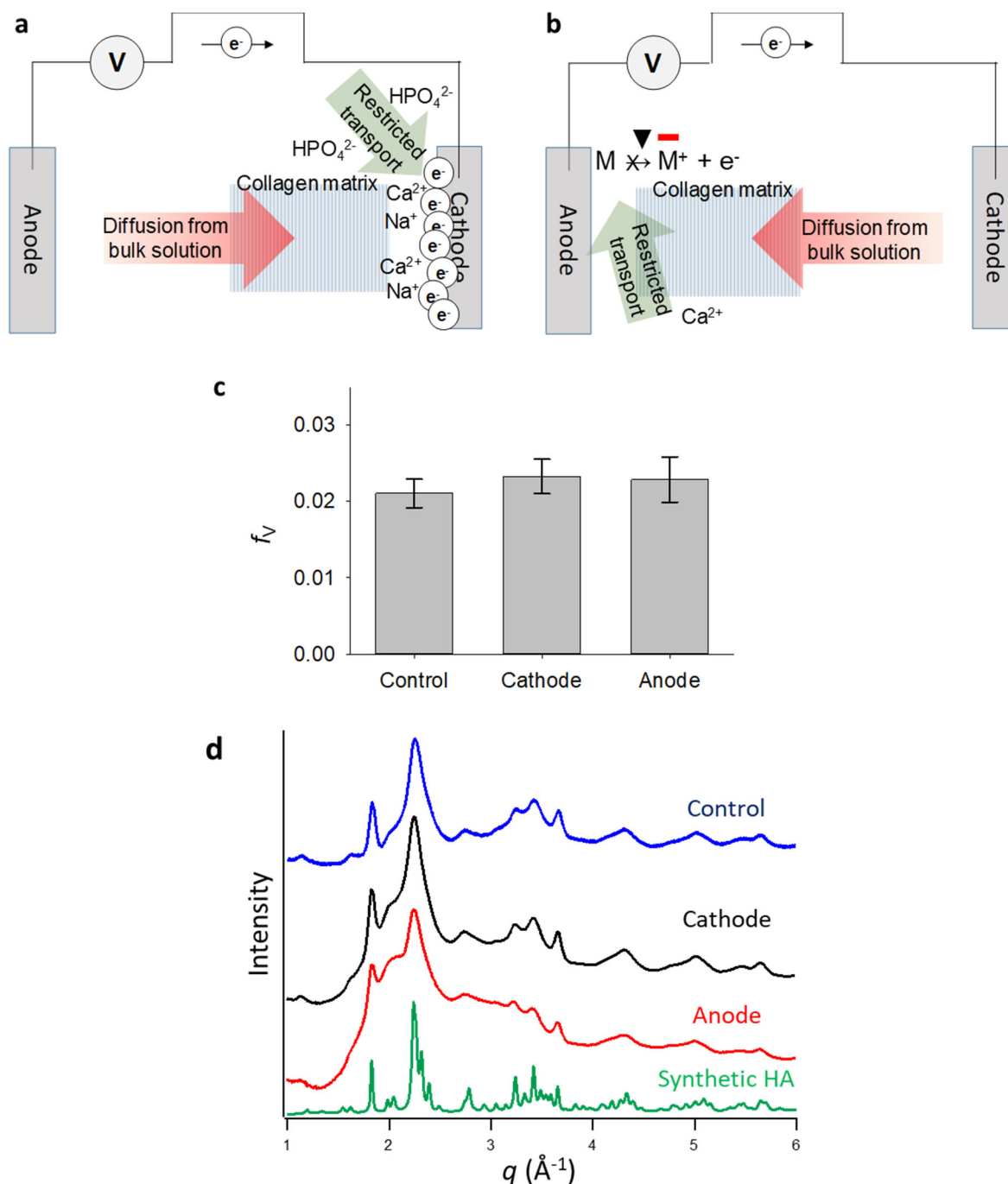


Figure S5. Collagen mineralization under continuous electrical stimulation (40 ± 0.5 mV). (a,b) Schematic of suggested mechanisms for collagen mineralization at the cathode and the anode. (c) Volume fractions of minerals, f_v , were evaluated from SAXS measurements after 48 h of mineralization. Error bars are standard errors ($n = 18$ for control and $n = 8$ for cathode and anode, respectively). (d) WAXD patterns of mineral formed in collagen after 16 h of mineralization.

Supporting References

1. Beaucage, G.; Kammler, H. K.; Pratsinis, S. E., Particle Size Distributions from Small-Angle Scattering using Global Scattering Functions. *J. Appl. Crystallogr.* **2004**, *37* (4), 523-535.
2. Li, Q.; Fernandez-Martinez, A.; Lee, B.; Waychunas, G. A.; Jun, Y.-S., Interfacial Energies for Heterogeneous Nucleation of Calcium Carbonate on Mica and Quartz. *Environ. Sci. Technol.* **2014**, *48* (10), 5745-5753.
3. Kim, D.; Lee, B.; Thomopoulos, S.; Jun, Y.-S., *In Situ* Evaluation of Calcium Phosphate Nucleation Kinetics and Pathways during Intra and Extrafibrillar Mineralization of Collagen Matrices. *Cryst. Growth Des.* **2016**, *16* (9), 5359-5366.
4. Ilavsky, J.; Jemian, P. R., Irena: Tool Suite for Modeling and Analysis of Small-Angle Scattering. *J. Appl. Crystallogr.* **2009**, *42* (2), 347-353.
5. Toby, B. H.; Von Dreele, R. B., GSAS-II: the genesis of a modern open-source all purpose crystallography software package. *J. Appl. Crystallogr.* **2013**, *46* (2), 544-549.